

## FULL PAPER

# Pd(0)- S-propyl-2-aminobenzothioate immobilized onto functionalized magnetic nanoporous MCM-41 as efficient and recyclable nanocatalyst for the Suzuki, Stille and Heck cross coupling reactions

Mohsen Nikoorazm<sup>1</sup>  | Farshid Ghorbani<sup>2</sup> | Arash Ghorbani-Choghamarani<sup>1</sup>  | Zahra Erfani<sup>1</sup>

<sup>1</sup>Department of Chemistry, Faculty of Science, Ilam University, P. O. Box 69315516, Ilam, Iran

<sup>2</sup>Department of Environment, Faculty of Natural Resource, University of Kurdistan, 66177-15177 Sanandaj, Iran

**Correspondence**

Mohsen Nikoorazm, Department of Chemistry, Faculty of Science, Ilam University, P.O. Box 69315516, Ilam, Iran.  
Email: e\_nikoorazm@yahoo.com

**Funding information**

Ilam University

The present work describes the use of Pd(0)- S-propyl-2-aminobenzothioate Complex immobilized onto functionalized magnetic nanoporous MCM-41(Fe<sub>3</sub>O<sub>4</sub>@MCM-41@Pd-SPATB) as efficient and recyclable nano-organometallic catalyst for C–C bond formation between various aryl halides with phenylboronic acid (Suzuki reaction), aryl halides with triphenyltin chloride (Stille reaction), and aryl halides with n-butyl acrylate (Heck reaction). All the reactions were carried out in PEG-400 as green solvent with short reaction time and good to excellent yields. This catalyst was characterized by FT-IR spectroscopy, XRD, TGA, VSM, ICP-OES, TEM, EDX and SEM techniques. Ease of operation, high efficiency, recovery and reusability for five continuous cycles without significant loss of its catalytic activities or metal leaching are the noteworthy features of the currently employed heterogeneous catalytic system.

**KEYWORDS**

C-C bond formation, Fe<sub>3</sub>O<sub>4</sub>@MCM-41@Pd-SPATB, heck reaction, Stille reaction, Suzuki reaction

## 1 | INTRODUCTION

Carbon–carbon coupling reactions such as the Suzuki–Miyaura, Stille and Heck–Mizoroki reactions have been widely used as significant procedures in modern synthetic organic chemistry for academic and industrial process including the pharmaceuticals, herbicides, agrochemicals, polymers, liquid crystal materials, hydrocarbons, UV screens, and advanced materials.<sup>[1–6]</sup> Mostly palladium complexes as efficient and active catalyst are used to catalyze these Carbon–carbon couplings reactions as they offer high product yields, high selectivity and compatibility with many functional moieties.<sup>[7]</sup> Homogeneous Pd catalysts are not used in industrial applications because of the difficulty in separating and recycling, and possibility of the high leaching of metal.<sup>[8–10]</sup> In order to solve this problem, new strategies should be employed.

In the past decade, the design of highly efficient and recyclable catalysts has become a very important matter for reasons of economic and environmental impact.<sup>[11]</sup> One strategy has focused on combining the high selectivity and activity of homogeneous catalysts with the ease of separation and recycling of heterogeneous catalysts.<sup>[12]</sup> For this aim, immobilization strategy used for linking homogeneous catalysts to various solid supports to facilitate catalysts separation and recycling, as well as product separation.<sup>[13]</sup> Among the different classes of supports available for this kind of catalysis, nanoparticle such as magnetic iron oxide and mesoporous silica material (especially MCM-41) are ideal heterogeneous supports. Because this type of supports can be used as efficiently bridge and fill the gap between homogeneous and heterogeneous catalysts.<sup>[14,15]</sup> More recently, the consolidation of functionalized mesoporous silica materials with

magnetic nanoparticles (MNPs), within a single material to develop novel porous magnetic nanostructure which have the advantages and properties of both mesoporous Silica (thermal and mechanical stability, large pore Volume and high surface area for catalyst loading) and magnetic nanoparticles (simple in synthesis, fast separation, low cost, high surface area and low toxicity), is undoubtedly of great interest for practical applications such as catalytic applications, magnetic storage and recording, for sensors, environmental, and biomedical applications.<sup>[16–20]</sup> Therefore owing to the context of reuse of palladium, Herein we report synthesis and spectroscopic characterization of a Pd-SPATB complex supported on functionalized magnetic nanostructured MCM-41 ( $\text{Fe}_3\text{O}_4@\text{MCM-41}@\text{Pd-SPATB}$ ), which has been applied as a novel and efficient nano-organometallic catalyst with excellent catalytic activity and selectivity in Carbon-carbon coupling reactions in PEG-400 as green solvent.

## 2 | EXPERIMENTAL

### 2.1 | Materials and techniques

The tetraethyl orthosilicate (TEOS), cationic surfactant cetyltrimethylammonium bromide (CTAB, 98 %), solvents and other materials were purchased from Sigma-Aldrich, Merck or Flucka Chemical Companies and were used as received without further purification.

Nanostructures were identified using a Holland Philips X'pert X-ray powder diffraction (XRD) diffractometer, with monochromatized Cu K $\alpha$  radiation under the conditions of 40 kV and 30 mA. Thermogravimetric analyses (TGA) of the samples were recorded between 30 - 800 °C using Shimadzu DTG-60 automatic thermal analyzer. Fourier transform infrared (FT-IR) spectra were recorded with FTIR spectrophotometer (Bruker, Germany) Vertex 70 in the range of 400 4000  $\text{cm}^{-1}$ . The particle size and morphology were examined using SEM with a FESEM-TESCAN MIRA3, and also using TEM with a High resolution TEM JEOL, JEM-2100F, 200KV transmission electron microscope. VSM measurements were performed using a vibrating sample magnetometer (VSM) MDKFD. The content of Pd was measured using inductively coupled plasma-optical emission spectrometry (ICP-OES).

### 2.2 | Synthesis of $\text{Fe}_3\text{O}_4@\text{MCM-41}$

The first, a mixture of  $\text{FeCl}_3 \cdot 6\text{H}_2\text{O}$  (2 g) and  $\text{FeCl}_2 \cdot 4\text{H}_2\text{O}$  (0.8 g) was dissolved in 10 ml of deionized water under  $\text{N}_2$  atmosphere. Then, the mixture was added to solution containing 100 ml of 1.0 mol  $\text{L}^{-1}$   $\text{NH}_3 \cdot \text{H}_2\text{O}$  and 0.4 g of cetyltrimethylammonium bromide (CTAB) under

sonication and  $\text{N}_2$  atmosphere. After the completed of the reaction for 30 min, the  $\text{Fe}_3\text{O}_4$  nanoparticles was isolated and dried at 80 °C in vacuum.<sup>[21]</sup> In the next step,  $\text{Fe}_3\text{O}_4$  nanoparticles (0.05 g) were dispersed in ethanol (20.0 ml) for 30 min using ultra sonication. Then, the suspension was centrifuged and the solid was in a mixture of  $\text{NH}_3$  (0.5 ml), deionized water (10 ml) and ethanol (20 ml). The system was kept under vigorous mechanical stirring for 30 min, and then (0.03 g) of TEOS was added dropwise. At the end of the addition, the mixture was kept under stirring at room temperature, for 6 h. The coated nanoparticles ( $\text{Fe}_3\text{O}_4@n\text{SiO}_2$ ) were separated with the aid of a magnet, and washed with ethanol and water several times. Then, the coated  $\text{Fe}_3\text{O}_4@n\text{SiO}_2$  nanoparticles were dispersed in a mixture of  $\text{NH}_3$  (0.6 ml), deionized water (40 ml), ethanol (30 ml) and CTAB (0.15 g). After stirring at room temperature for 30 min, 0.4 g of TEOS, added slowly to the solution and continued to stir for 6 h. The solid products were collected by magnetic separation, washed with plenty of ethanol/deionized water, and subsequently dried in a vacuum oven at 80 °C for 12 h. After this period, to remove organic template CTAB, ethanol (100 ml) and 5 ml of 2 mol  $\text{L}^{-1}$  HCl was added to the 0.1 g of produced nanocomposite, then the mixture was kept under stirring at room temperature, for 48 h. The solid products were collected by magnetic separation, and subsequently dried in a vacuum oven at 80 °C for 24 h. Finally, we obtained the  $\text{Fe}_3\text{O}_4@\text{MCM-41}$ .

### 2.3 | Preparation of MPTMS functionalized mag mesoporous silica ( $\text{Fe}_3\text{O}_4@\text{MCM-41-SH}$ )

To a suspension of  $\text{Fe}_3\text{O}_4@\text{MCM-41}$  (4.8 g, 80 °C) in *n*-hexane, 4.8 g of (3-mercaptopropyl) trimethoxysilane (MPTMS) was added slowly and then refluxed for 24 h. The separated solid was collected by magnetic separation, washed with *n*-hexane and dried under vacuum.

### 2.4 | Preparation of heterogeneous Pd-SPATB complex immobilized onto magnetic nanoporous MCM-41 ( $\text{Fe}_3\text{O}_4@\text{MCM-41}@\text{Pd-SPATB}$ )

For the preparation of  $\text{Fe}_3\text{O}_4@\text{MCM-41}@\text{Pd-SPATB}$ , 0.5 g of functionalized  $\text{Fe}_3\text{O}_4@\text{MCM-41}$  and S-propyl-2-aminobenzothioate (1.2 mmol) in ethanol was refluxed for 3 h. The resulting solid was washed with ethanol, collected by magnetic separation and dried under vacuum and designated as  $\text{Fe}_3\text{O}_4@\text{MCM-41}@\text{SPATB}$ . Ultimately, the  $\text{Fe}_3\text{O}_4@\text{MCM-41}@\text{Pd-SPATB}$  was prepared by stirring a mixture of Pd (OAc)<sub>2</sub> (0.168 g, 0.63 mmol) and 0.250 g  $\text{Fe}_3\text{O}_4@\text{MCM-41}@\text{SPATB}$  in ethanol (20 ml) for

20 h under reflux conditions. Afterward, For the reduction of Pd(II) present in the resulting catalyst, NaBH<sub>4</sub> (0.022 g, 0.057 mmol) was added and then refluxed under the same conditions for 2 h. The final product was separated by magnet, and washed with ethanol and dried at room temperature. The detailed preparation route for Fe<sub>3</sub>O<sub>4</sub>@MCM-41@Pd-SPATB is shown in Scheme 1.

## 2.5 | General procedure for the synthesis of biphenyl derivatives

A mixture of an aryl halide (1 mmol), phenylboronic acid or Ph<sub>3</sub>SnCl (0.5 mmol), K<sub>2</sub>CO<sub>3</sub> (3 mmol), and Fe<sub>3</sub>O<sub>4</sub>@MCM-41@Pd-SPATB was added to a reaction vessel. The resulting mixture was stirred in PEG-400 at 80 °C for an appropriate time and the progress of the reaction was monitored by thin-layer chromatography (TLC). After completion of the reaction, the catalyst was separated using an external magnet and washed with ethyl acetate. The reaction mixture was extracted with ethyl acetate and H<sub>2</sub>O, and dried over anhydrous Na<sub>2</sub>SO<sub>4</sub> (1.5 g). Then the solvent was evaporated and pure Biphenyl derivatives were obtained in good to excellent yields.

## 2.6 | General procedure for the synthesis of butyl Cinnamate derivatives

A mixture of aryl halide (1 mmol), an butyl acrylate (1.2 mmol), K<sub>2</sub>CO<sub>3</sub> (3 mmol), and Fe<sub>3</sub>O<sub>4</sub>@MCM-41@Pd-SPATB (0.006 g, 0.94 mol%) was stirred in PEG-400 at 120 °C for an appropriate time and progress of the reaction was monitored using TLC. After completion of the reaction, the mixture was cooled down to room

temperature. Then catalyst was separated by an external magnet and the reaction mixture was extracted with diethyl ether and water. The organic layer was dried over Na<sub>2</sub>SO<sub>4</sub> (1.5 g) and after evaporation of the diethyl ether, the pure product was obtained.

## 2.7 | Selected spectral data

**4-methoxy-1,1'-biphenyl** (Table 2, entry 4): <sup>1</sup>H NMR (400 MHz, CDCl<sub>3</sub>): δ<sub>H</sub>= 7.65-7.54 (m, 4H), 7.47-7.43 (t, *J*= 7.6 Hz, 2H), 7.36-7.29 (tt, *J*= 7.6, 1.2 Hz, 1H), 7.03-7.01 (dt, *J*= 8.8, 2.4 Hz, 2H), 3.89 (s, 3H) ppm.

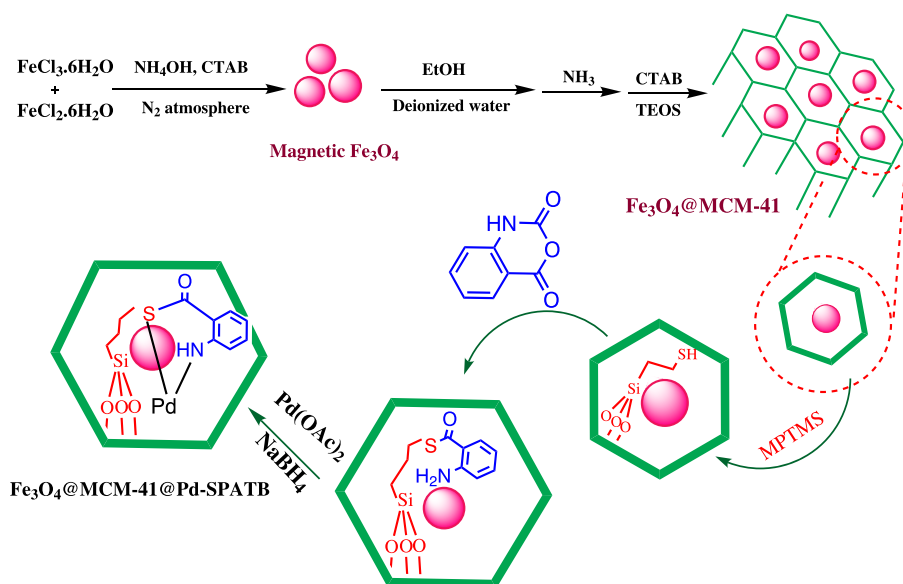
**butyl 3-(p-tolyl)acrylate** (Table 6, entry 2):: <sup>1</sup>H NMR (400 MHz, CDCl<sub>3</sub>): δ<sub>H</sub>= 7.69-7.65 (d, *J*= 16 Hz, 1H), 7.49-7.47 (d, *J*= 8 Hz, 2H), 7.25-7.23 (d, *J*= 8 Hz, 2H), 6.47-6.43 (d, *J*= 16 Hz, 1H), 4.27-4.24 (t, *J*= 6.6 Hz, 2H), 2.43 (s, 3H), 1.78-1.71 (m, 2H), 1.52-1.46 (m, 2H), 0.99 (t, *J*= 7.6 Hz, 3H) ppm.

## 3 | RESULT AND DISCUSSION

### 3.1 | Characterization of Fe<sub>3</sub>O<sub>4</sub>@MCM-41@Pd-SPATB

The structure of Pd(0)- SPATB complex anchored on to the surface of magnetic MCM-41 (Fe<sub>3</sub>O<sub>4</sub>@MCM-41@Pd-SPATB) as a novel and recyclable heterogeneous nanocatalyst was studied and fully characterized by FT-IR, XRD, EDS, TEM, SEM, VSM, and TGA analysis.

The SEM images of Fe<sub>3</sub>O<sub>4</sub>@MCM-41 and Fe<sub>3</sub>O<sub>4</sub>@MCM-41@Pd-SPATB are shown in Figure 1. As shown in these images, the morphologies of the Fe<sub>3</sub>O<sub>4</sub>@MCM-41 and Fe<sub>3</sub>O<sub>4</sub>@MCM-41@Pd-SPATB are



**SCHEME 1** Synthesis of Fe<sub>3</sub>O<sub>4</sub>@MCM-41@Pd-SPATB

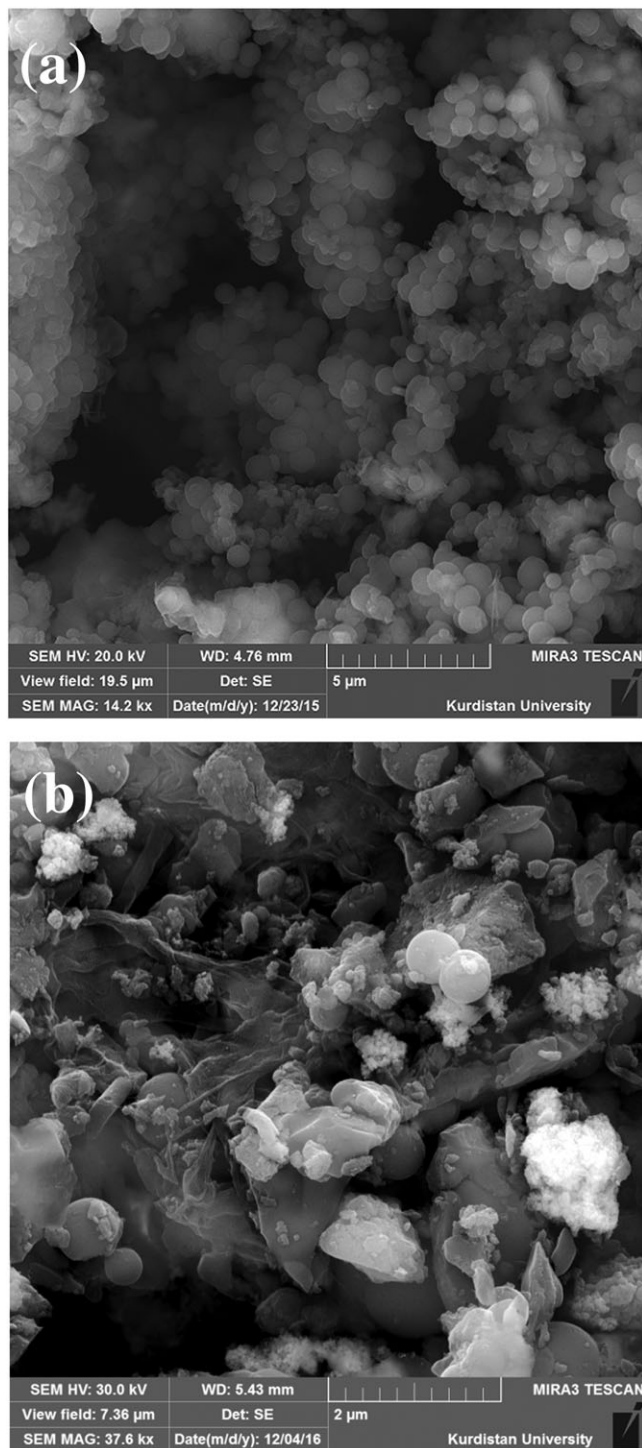


**FIGURE 1** (a) SEM images of Fe<sub>3</sub>O<sub>4</sub>@MCM-41 and (b) Fe<sub>3</sub>O<sub>4</sub>@MCM-41@Pd-SPATB

agglomerations of small spherical regular particles with uniform nanometer sized.

The energy dispersive spectrum (EDS) evidently shows the presence of Pd, Fe, Si, O, N, S and C species in the catalyst (Figure 2).

HR TEM images of the Fe<sub>3</sub>O<sub>4</sub>@MCM-41@Pd-SPATB are shown in Figure 3. Based on the TEM micrograph,

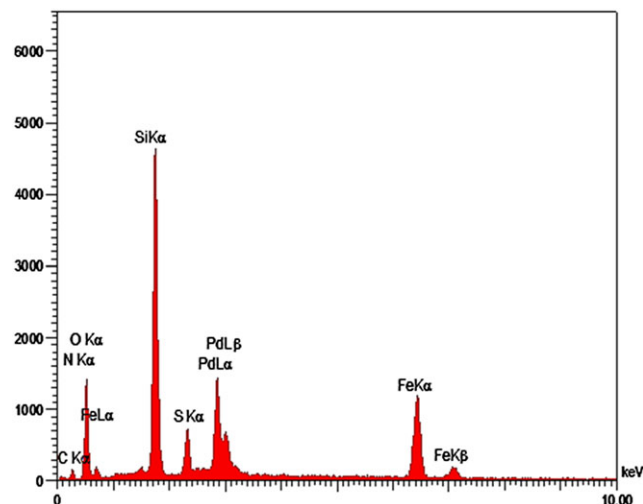
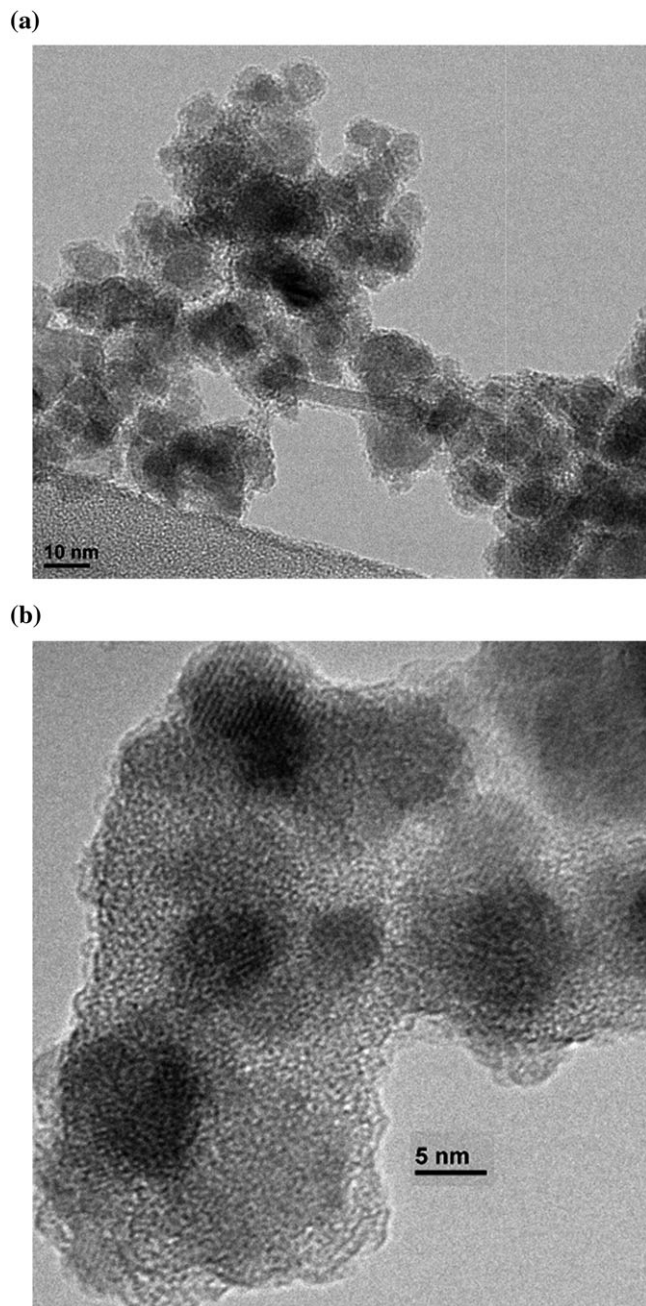


**FIGURE 2** The EDS spectrum of Fe<sub>3</sub>O<sub>4</sub>@MCM-41@Pd-SPATB

analysis of Fe<sub>3</sub>O<sub>4</sub>@MCM-41@Pd-SPATB surface morphology demonstrated the well-ordered mesostructures with uniform pore dimension and hexagonal structure and agglomeration of many ultrafine spherical like particles which display dark magnetite cores surrounded by a shell.

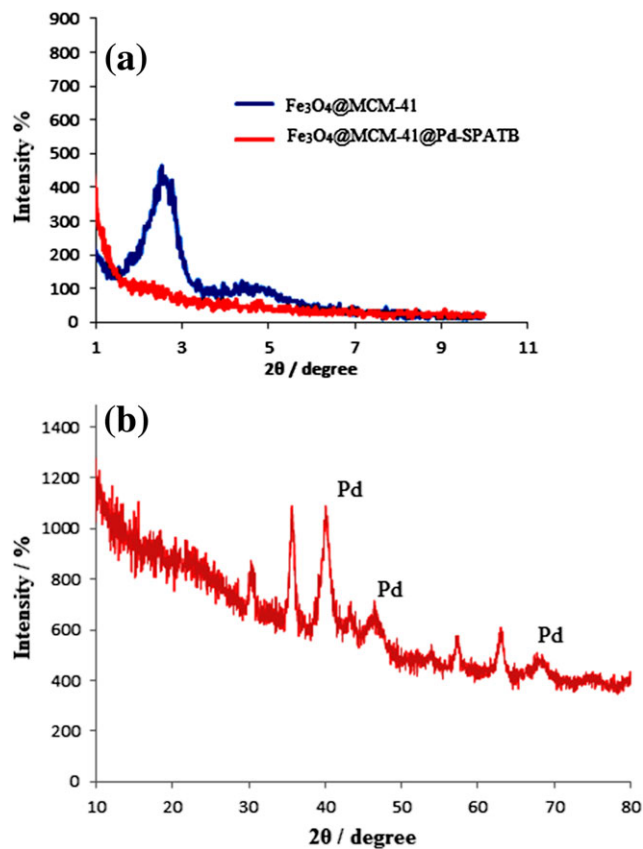
The XRD patterns of Fe<sub>3</sub>O<sub>4</sub>@MCM-41 and Fe<sub>3</sub>O<sub>4</sub>@MCM-41@Pd-SPATB are shown in Figure 4. As seen from the small-angle XRD patterns in Figure 4a, The XRD pattern of Fe<sub>3</sub>O<sub>4</sub>@MCM-41 shows a very intense reflection at  $2\theta = 2.36^\circ$  for  $d_{100}$  plane and also two additional high order peaks with low intensity reflections at  $2\theta = 3.95^\circ$  and  $4.39^\circ$  for  $d_{110}$  and  $d_{200}$  planes respectively, typically confirming the presence of ordered hexagonal mesoporous structure of MCM-41.<sup>[21]</sup> The wide-angle XRD for the Fe<sub>3</sub>O<sub>4</sub>@MCM-41@Pd-SPATB sample are shown in Figure 4 b. The characteristic peaks at  $2\theta = 30.25^\circ, 35.6^\circ, 43.8^\circ, 53.9^\circ, 57.0^\circ$  and  $62.8^\circ$  assigned to magnetite were observable for samples which agrees with the standard Fe<sub>3</sub>O<sub>4</sub> (cubic phase) XRD spectrum and demonstrated that catalyst had been successfully synthesized without damaging the crystal structure of Fe<sub>3</sub>O<sub>4</sub>.<sup>[13]</sup> The broad peak at  $2\theta = 20\text{--}30^\circ$  corresponds to amorphous silica, which indicates that the silica is successfully coated on the surface of the Fe<sub>3</sub>O<sub>4</sub> nanoparticles.<sup>[49]</sup> Also the XRD pattern of Fe<sub>3</sub>O<sub>4</sub>@MCM-41@Pd-SPATB exhibits a series of peaks ( $39.9^\circ, 46.4^\circ$  and  $67.5^\circ$ ) which are indexed to Pd(0) on the surface of Fe<sub>3</sub>O<sub>4</sub>@MCM-41.<sup>[28]</sup> The comparison study of small-angle XRD patterns of Fe<sub>3</sub>O<sub>4</sub>@MCM-41 and Fe<sub>3</sub>O<sub>4</sub>@MCM-41@Pd-SPATB shows that after grafting of Pd through complex formation into Fe<sub>3</sub>O<sub>4</sub>@MCM-41, the reflections with weaker intensities are observed.

Figure 5 shows FT-IR spectra of (a) Fe<sub>3</sub>O<sub>4</sub> (b) Fe<sub>3</sub>O<sub>4</sub>@MCM-41 (c) Fe<sub>3</sub>O<sub>4</sub>@MCM-41@nPr-SH (d) Fe<sub>3</sub>O<sub>4</sub>@MCM-41@SPATB and (e) Fe<sub>3</sub>O<sub>4</sub>@MCM-41@Pd-



**FIGURE 3** The HR TEM micrographs of  $\text{Fe}_3\text{O}_4@MCM-41@Pd-SPATB$

SPATB respectively. The FT-IR spectrum of the  $\text{Fe}_3\text{O}_4$  nanoparticles (spectrum a) shows the strong absorptions near  $579$  and  $444\text{ cm}^{-1}$  and  $3000\text{--}3500\text{ cm}^{-1}$  due to Fe–O and O–H stretching vibrations,<sup>[29]</sup> for the  $\text{Fe}_3\text{O}_4@MCM-41$  sample (spectrum b) the peaks at  $3445\text{ cm}^{-1}$  is due to the stretching vibrating absorption of O–H band in the surfaced hydroxyl groups, also three characteristic peaks at  $460\text{ cm}^{-1}$ ,  $958\text{ cm}^{-1}$  and  $1081\text{ cm}^{-1}$  corresponded to bending, symmetric stretching and asymmetric stretching, Si–O–Si vibrations respectively.<sup>[30]</sup> Immobilization of MPTMS



**FIGURE 4** XRD patterns of (a) small angle of  $\text{Fe}_3\text{O}_4@MCM-41$  and  $\text{Fe}_3\text{O}_4@MCM-41@Pd-SPATB$  and (b) wide angle of  $\text{Fe}_3\text{O}_4@MCM-41@Pd-SPATB$

on the surface of  $\text{Fe}_3\text{O}_4@MCM-41$  was indicated by the appearance of two peaks at  $2981$  and  $2936\text{ cm}^{-1}$ , assigned to the C–H stretching vibrations, also S–H stretching vibration modes as a weak band that appears at  $2450\text{ cm}^{-1}$  (Figure 5c). Reaction of S-propyl-2-aminobenzothioate with SH immobilized on  $\text{Fe}_3\text{O}_4@MCM-41$  produces  $\text{Fe}_3\text{O}_4@MCM-41@ATBA$  in which the presence of carbonyl group is indicated by the  $1623\text{ cm}^{-1}$  band in its FT-IR spectrum (Figure 5d). Figure 5(e) shows the FT-IR spectrum after covalent bonding of Pd ions onto  $\text{Fe}_3\text{O}_4@MCM-41@SPATB$  the broad band in the range  $1400\text{--}1650\text{ cm}^{-1}$  is attributed to the formation of palladium complex.<sup>[1]</sup>

The superparamagnetic property of  $\text{Fe}_3\text{O}_4@MCM-41$  (a) and  $\text{Fe}_3\text{O}_4@MCM-41@Pd-SPATB$  (b) were investigated using VSM at room temperature (Figure 6). VSM measurements for  $\text{Fe}_3\text{O}_4@MCM-41$  nanoparticles show that the saturation magnetization ( $M_s$ ) is  $13.02\text{ emu g}^{-1}$  Figure 6 (a), while  $M_s$  of  $\text{Fe}_3\text{O}_4@MCM-41@Pd-SPATB$  is decreased to  $12.11\text{ emu g}^{-1}$  Figure 6 (b). On the basis of these results, the successful grafting of organic layers including palladium complex on  $\text{Fe}_3\text{O}_4@MCM-41$  is verified.<sup>[31]</sup>

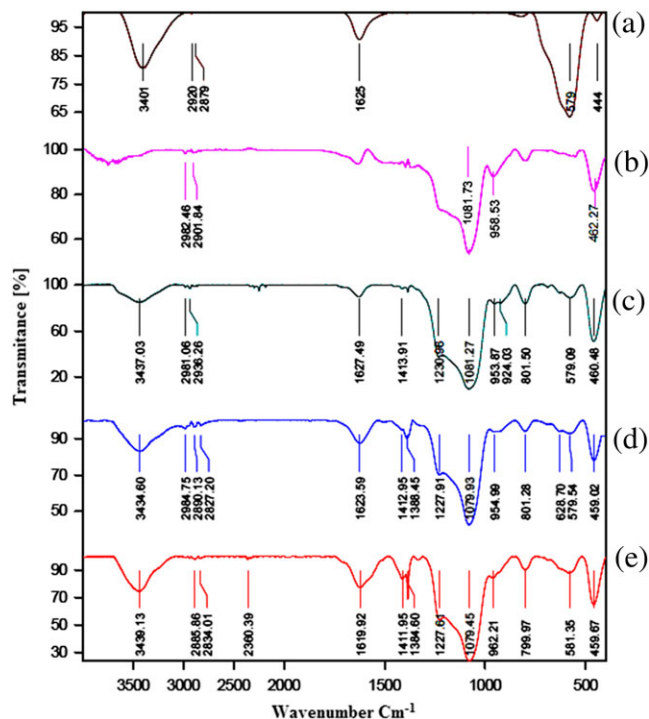


**FIGURE 5** FT-IR spectra of (a)  $\text{Fe}_3\text{O}_4$  (b)  $\text{Fe}_3\text{O}_4@MCM-41$  (c)  $\text{Fe}_3\text{O}_4@MCM-41@nPr-SH$  (d)  $\text{Fe}_3\text{O}_4@MCM-41@SPATB$  and (e)  $\text{Fe}_3\text{O}_4@MCM-41@Pd-SPATB$ .

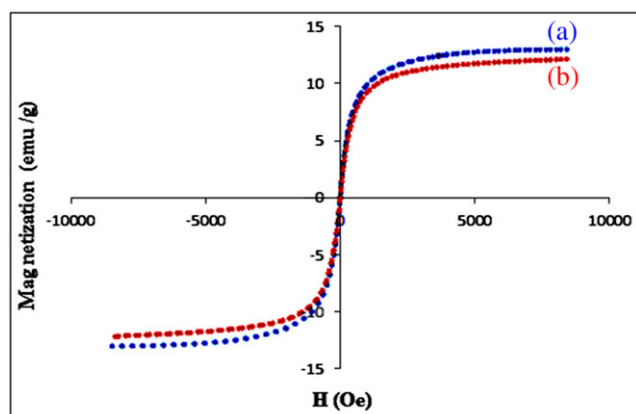


**FIGURE 6** Magnetic curves of (a)  $\text{Fe}_3\text{O}_4@MCM-41$  and (b)  $\text{Fe}_3\text{O}_4@MCM-41@Pd-SPATB$

The thermogravimetric analysis (TGA) curves of  $\text{Fe}_3\text{O}_4@MCM-41$  and  $\text{Fe}_3\text{O}_4@MCM-41@Pd-SPATB$  are shown in Figure 7. The TGA of the synthesized  $\text{Fe}_3\text{O}_4@MCM-41$  shows 3 % weight loss in one step at between 25 to 100 °C due to desorption of water.  $\text{Fe}_3\text{O}_4@MCM-41@Pd-SPATB$  sample showed a mass loss about 5.6 % below 250 °C due to the removal of physically adsorbed solvent and surface hydroxyl groups, the other weight loss is in the region of 250–650 °C (about 15 %) mainly related to the decomposition of immobilized organic moieties on the  $\text{Fe}_3\text{O}_4@MCM-41@Pd-SPATB$  surface,<sup>[32]</sup> and the third weight loss (about 11%) appears

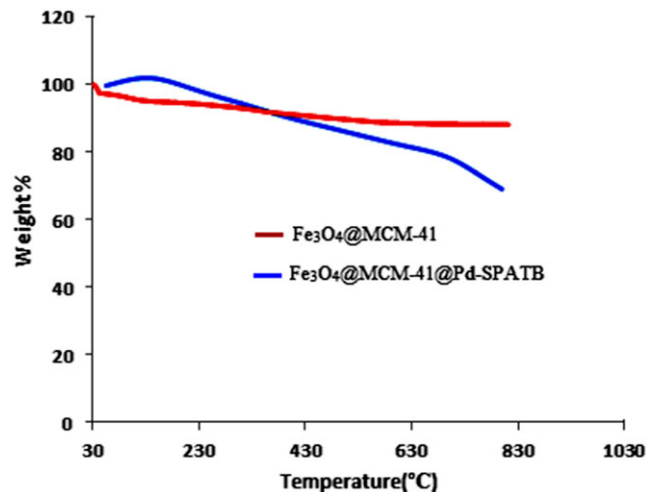


**FIGURE 7** TGA thermograms of  $\text{Fe}_3\text{O}_4@MCM-41$  and  $\text{Fe}_3\text{O}_4@MCM-41@Pd-SPATB$

at above 650 °C as a result of the condensation of the silanol groups.

Finally, to determine the exact amount of Pd in  $\text{Fe}_3\text{O}_4@MCM-41@Pd-SPATB$ , ICP-OES was used. From this analysis, the Pd amount of the immobilized catalyst on  $\text{Fe}_3\text{O}_4@MCM-41$  was found to be  $1.59 \times 10^{-3}$  mol/g.

### 3.2 | Evaluation of the catalytic activity of $\text{Fe}_3\text{O}_4@MCM-41@Pd-SPATB$ in Suzuki-Miyaura, Stille and Mizoroki-heck reactions

After full characterization of the catalyst structure, the catalytic activity of this magnetic mesoporous compound was examined in C–C coupling reactions, namely Suzuki, Stille and Heck reactions. At the onset of our work, the catalytic activity of complex was investigated in Suzuki–Miyaura cross coupling reactions. For this propose the reaction between iodobenzene (1 mmol) with phenyl boronic acid (1 mmol) using  $\text{K}_2\text{CO}_3$  as a base at 80 °C was chosen as model reaction and the effects of various parameters such as amount of catalyst, solvent, temperature and base were studied for this model reaction (Table 1).

When the reaction was carried out in the absence of catalyst, the desired product was not achieved after 6 h (Table 1, entry 1). Thus, we tested different amount of catalyst (Table 1, entries 2–4) and the best amount of catalyst was found 4 mg (0.63 mol %) for this reaction (Table 1, entry 3). In the next step, the influence of various solvents, PEG-400,  $\text{H}_2\text{O}$ , THF, Toluene, DMSO, EtOH, DMF, and 1,4-Dioxan at 80 °C was studied (Table 1, entries 4–11). The best results are obtained for PEG-400. Then, we investigated the effects of bases on the reaction in PEG-400 solvent. The different bases

**TABLE 1** Optimization of the solvent, base, temperature and concentration of catalyst for the synthesis of biphenyl in Suzuki reaction

Entry	Temperature (°C)	Solvent	Base	Catalyst amount (mg)	Time (min)	Yield <sup>a</sup>
1	80	PEG-400	K <sub>2</sub> CO <sub>3</sub>	-	360	Trace
2	80	PEG-400	K <sub>2</sub> CO <sub>3</sub>	5	25	94
3	80	PEG-400	K <sub>2</sub> CO <sub>3</sub>	4	25	94
4	80	PEG-400	K <sub>2</sub> CO <sub>3</sub>	3	25	82
5	80	1,4-dioxane	K <sub>2</sub> CO <sub>3</sub>	4	25	20
6	80	DMSO	K <sub>2</sub> CO <sub>3</sub>	4	25	72
7	80	Toluene	K <sub>2</sub> CO <sub>3</sub>	4	25	16
8	80	THF	K <sub>2</sub> CO <sub>3</sub>	4	25	39
9	80	H <sub>2</sub> O	K <sub>2</sub> CO <sub>3</sub>	4	25	25
10	80	DMF	K <sub>2</sub> CO <sub>3</sub>	4	25	92
11	80	EtOH	K <sub>2</sub> CO <sub>3</sub>	4	25	82
12	80	PEG-400	Et <sub>3</sub> N	4	25	92
13	80	PEG-400	NaHCO <sub>3</sub>	4	25	83
14	80	PEG-400	Na <sub>2</sub> CO <sub>3</sub>	4	25	88
15	80	PEG-400	KOH	4	25	Trace
16	60	PEG-400	K <sub>2</sub> CO <sub>3</sub>	4	25	90
17	40	PEG-400	K <sub>2</sub> CO <sub>3</sub>	4	25	68
18	25	PEG-400	K <sub>2</sub> CO <sub>3</sub>	4	25	30

Reaction conditions: iodobenzene (1 mmol), phenyl boronic acid (1 mmol), base (3 mmol), Fe<sub>3</sub>O<sub>4</sub>@MCM-41@Pd-SPATB (4 mg, 0.63 mol%) and PEG-400 (2 ml)

<sup>a</sup>Isolated yield.

including NaHCO<sub>3</sub>, KOH, (Et)<sub>3</sub>N, Na<sub>2</sub>CO<sub>3</sub> and K<sub>2</sub>CO<sub>3</sub> were studied (Table 1, entries 3, 12–15). High yield and shorter reaction time are obtained when K<sub>2</sub>CO<sub>3</sub> is employed as base, therefore, we chose K<sub>2</sub>CO<sub>3</sub> as the base in all of the coupling reactions. Also, the effect of temperature was studied (Table 1, entries 3, 16–18). Optimum reaction conditions base on the effect of temperature shows that excellent yield of the product is obtained at 80 °C. Therefore, the best result was obtained when the reaction was carried out with Fe<sub>3</sub>O<sub>4</sub>@MCM-41@Pd-SPATB (0.004 g), iodobenzene (1 mmol), phenyl boronic acid (1 mmol) and K<sub>2</sub>CO<sub>3</sub> (3 mmol) in PEG-400 at 80 °C (Table 1, entry 3).

To examine the utility and generality of this approach, various aryl halides were reacted with phenyl boronic acid in the optimal reaction conditions for the synthesis of a wide variety of biphenyls. The biphenyl derivatives were obtained in high yields and short reaction time (Table 2). As shown in Table 2, completion of the reaction involving chlorobenzene was slower than for iodobenzene or bromobenzene and requires more amount of Fe<sub>3</sub>O<sub>4</sub>@MCM-41@Pd-SPATB (8 mg) and higher temperature (100 °C) (Table 2, entries 11–13).

Also, we examined the catalytic activity of Fe<sub>3</sub>O<sub>4</sub>@MCM-41@Pd-SPATB in the Stille cross-coupling reactions. In order to find out the best reaction conditions,

the reaction between the iodobenzene (1.0 mmol) and Ph<sub>3</sub>SnCl (0.5 mmol) in the presence of base (3 mmol) was probed as a model reaction. The catalytic reactions were first carried out in the absence of catalyst, which did not give a quantitative yield of products after 10 h (Table 3, entry 1).

To investigate the effect of the catalyst, systematic studies were carried out in the presence of different amounts of the catalyst in PEG (Table 3, entries 2–4). The best result is observed with 6 mg (0.94 mol%) of Fe<sub>3</sub>O<sub>4</sub>@MCM-41@Pd-SPATB (Table 3, entry 4). Also, the effect of a series of bases on the activity of Fe<sub>3</sub>O<sub>4</sub>@MCM-41@Pd-SPATB catalyst was studied and K<sub>2</sub>CO<sub>3</sub> was selected as the proper base (Table 3, entries 5–8). Beside, in order to find appropriate solvent, several solvents were also tested (Table 3, entries 9–14) among them PEG-400 gives the best result. Further optimization was performed at different temperatures (Table 3, entries 15–17). A high yield of product can be achieved at 80 °C.

After optimization, the Stille reaction of aryl halides with Ph<sub>3</sub>SnCl in the presence of Fe<sub>3</sub>O<sub>4</sub>@MCM-41@Pd-SPATB (6 mg, 0.94 mol%) in PEG-400 at 80 °C were carried out and the obtained results are listed in Table 4.

Catalytic cycle for Suzuki and Stille reaction in the presence of Fe<sub>3</sub>O<sub>4</sub>@MCM-41@Pd-SPATB was outlined in Scheme 2.

**TABLE 2** C–C coupling of aryl halides with phenylboronic acid in the presence of  $\text{Fe}_3\text{O}_4@\text{MCM-41}@\text{Pd-SPATB}$  (4 mg, 0.63 mol%) in PEG at 80 °C

$\text{Ar-X} + \text{Ph-B(OH)}_2 \xrightarrow[\text{K}_2\text{CO}_3, \text{PEG}, 80^\circ\text{C}]{\text{Fe}_3\text{O}_4@\text{MCM-41}@\text{Pd-SPATB}} \text{Ar-Ph}$

X = I, Br, Cl

Entry	Aryl halide	Time (min)	Yield (%) <sup>a</sup>	TOF (h <sup>-1</sup> )	Melting point (°C)
1		25	94	355.2	65-67 [22]
2		45	95	201.05	45-47 [23]
3		40	96	228.8	Oil [22]
4		60	93	147.6	82-84 [22]
5		50	92	175.3	67-68 [22]
6		45	93	196.8	42-44 [22]
7		60	90	142.8	81-83 [22]
8		45	94	198.94	79-81 [22]
9		60	93	147.6	113-114 [24]
10		60	92	146.03	70-72 [22]
11 <sup>b</sup>		90	90	95.2	64-66 [23]
12 <sup>b</sup>		200	88	41.9	81-83 [22]
13 <sup>b</sup>		240	90	35.7	111-113 [23]

<sup>a</sup>Isolated yield.<sup>b</sup>Conditions were as follows:  $\text{Fe}_3\text{O}_4@\text{MCM-41}@\text{Pd-SPATB}$  (8 mg, 1.26 mol%) at 100 °C.

In order to extend the general application of the  $\text{Fe}_3\text{O}_4@\text{MCM-41}@\text{Pd-SPATB}$  as a catalyst, the ability of this catalyst was investigated for C–C coupling through the Heck reaction. The reaction of iodobenzene with *n*-butyl acrylate have been employed as the model reaction. The effect of the amount of catalyst, solvent (EtOH, H<sub>2</sub>O, Toluene, DMSO, DMF, 1, 4-Dioxan and PEG), the nature of the base (KOH, Et<sub>3</sub>N, NaHCO<sub>3</sub>, K<sub>2</sub>CO<sub>3</sub> or Na<sub>2</sub>CO<sub>3</sub>) and temperature (room temperature to 120 °C), on the outcome of the coupling of iodobenzene with *n*-butyl acrylate was examined. A summary of the results is shown in Table 5. As shown in Table 5 entry 1, the reaction did not occur in the absence of  $\text{Fe}_3\text{O}_4@\text{MCM-41}@\text{Pd-SPATB}$ . Among the different amount of catalyst tested, (6 mg, 0.94 mol%) was found to be the most effective catalytic amount since it gave the highest yield of the product (Tables 5, entry 4). Among the different solvents, the best yield is found in the presence of PEG-400 (Table 5, entry 4). Also, the reaction was significantly affected by the nature of base and Using K<sub>2</sub>CO<sub>3</sub> as a base, the

reaction had proceeded in high yield. Finally, different temperatures were examined for the model reaction (Table 5, entries 13–16) and high conversion of product was achieved at 120 °C.

After the optimization of the reaction conditions, the reaction of various aryl halide derivatives with *n*-butyl acrylate was then investigated to confirm the generality of the present method. The results of this study are summarized in Table 6.

Catalytic cycle for Heck reaction in the presence of  $\text{Fe}_3\text{O}_4@\text{MCM-41}@\text{Pd-SPATB}$  was outlined in Scheme 3.

The recovery and reusability of the catalysts is an important factor in green chemistry and heterogeneous catalysis. In another investigation, the recovery and reusability of the  $\text{Fe}_3\text{O}_4@\text{MCM-41}@\text{Pd-SPATB}$  was investigated in the Suzuki–Miyaura reaction from iodobenzene (1 mmol) with phenylboronic acid (1 mmol), K<sub>2</sub>CO<sub>3</sub> (3 mmol),  $\text{Fe}_3\text{O}_4@\text{MCM-41}@\text{Pd-SPATB}$  (4 mg, 0.63 mol%) in PEG at 80 °C, Still reaction from iodobenzene (1 mmol) with Ph<sub>3</sub>SnCl (0.5 mmol), K<sub>2</sub>CO<sub>3</sub>

**TABLE 3** Catalytic results for the Stille reaction

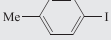
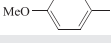
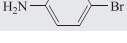
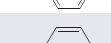
Entry	Temperature (°C)	Solvent	Base	Catalyst (mg)	Time(min)	Yield <sup>a</sup>
1	80	PEG-400	K <sub>2</sub> CO <sub>3</sub>	-	600	- <sup>b</sup>
2	80	PEG-400	K <sub>2</sub> CO <sub>3</sub>	4	40	76
3	80	PEG-400	K <sub>2</sub> CO <sub>3</sub>	5	40	84
4	80	PEG-400	K <sub>2</sub> CO <sub>3</sub>	6	40	92
5	80	PEG-400	NaHCO <sub>3</sub>	6	40	90
6	80	PEG-400	Et <sub>3</sub> N	6	40	90
7	80	PEG-400	KOH	6	40	Trace
8	80	PEG-400	Na <sub>2</sub> CO <sub>3</sub>	6	40	90
9	80	EtOH	K <sub>2</sub> CO <sub>3</sub>	6	40	Trace
10	80	DMSO	K <sub>2</sub> CO <sub>3</sub>	6	40	30
11	80	Toluene	K <sub>2</sub> CO <sub>3</sub>	6	40	-
12	80	THF	K <sub>2</sub> CO <sub>3</sub>	6	40	15
13	80	1,4-dioxane	K <sub>2</sub> CO <sub>3</sub>	6	40	-
14	80	H <sub>2</sub> O	K <sub>2</sub> CO <sub>3</sub>	6	40	77
15	70	PEG-400	K <sub>2</sub> CO <sub>3</sub>	6	40	78
16	60	PEG-400	K <sub>2</sub> CO <sub>3</sub>	6	40	44
17	25	PEG-400	K <sub>2</sub> CO <sub>3</sub>	6	40	-

The reaction mixture consisted of aryl halide (1.0 mmol), Ph<sub>3</sub>SnCl (0.5 mmol), base (3 mmol), catalyst and 2 ml of solvent. Reaction time was 40 min.

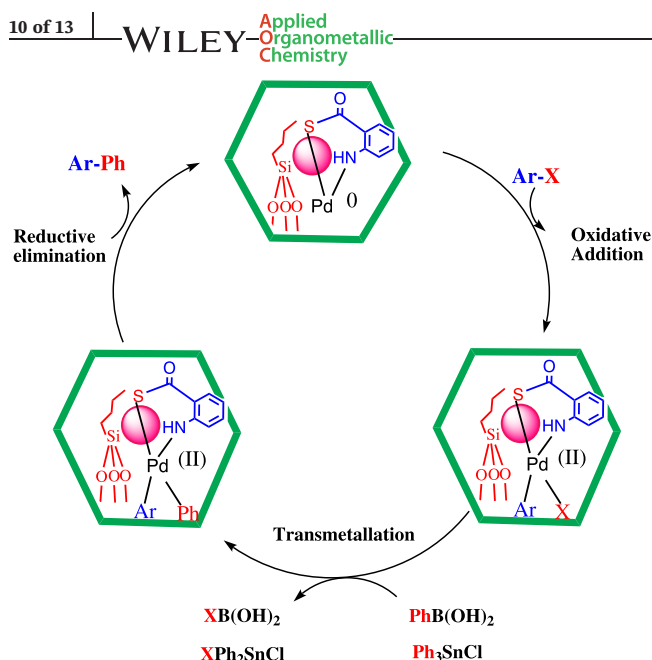
<sup>a</sup>Isolated yield.

<sup>b</sup>No reaction.

**TABLE 4** The Stille reaction of aryl halides with Ph<sub>3</sub>SnCl in the presence of Fe<sub>3</sub>O<sub>4</sub>@MCM-41@Pd-SPATB (6 mg, 0.94 mol%) in PEG at 80 °C

Entry	Aryl halide	Time (min)	Yield (%) <sup>a</sup>	TOF (h <sup>-1</sup> )	Melting point (°C)
1		40	94	150.1	64-66 [22]
2		45	93	131.9	45-47 [23]
3		55	88	102.8	83-85 [22]
4		85	84	63.3	53-55 [22]
5		55	90	105.2	63-66 [22]
6		70	88	80.7	42-44 [22]
7		75	87	70.04	81-83 [22]
8		120	89	47.3	80-82 [22]
9		80	93	74.2	112-114 [23]
10		140	89	40.5	71-73 [22]

<sup>a</sup>Isolated yield.



**SCHEME 2** Possible mechanism of Suzuki and Stille coupling reactions

(3 mmol),  $\text{Fe}_3\text{O}_4\text{@MCM-41@Pd-SPATB}$  (6 mg, 0.94 mol%) in PEG at 80 °C and Heck–Mizoroki cross-coupling reactions from iodobenzene (1 mmol) and butyl acrylate (1.2 mmol),  $\text{K}_2\text{CO}_3$  (3 mmol),  $\text{Fe}_3\text{O}_4\text{@MCM-41@Pd-SPATB}$  (6 mg, 0.94 mol%) in PEG at 120 °C. After completion of the reaction, the reaction mixture was cooled to room temperature, the catalyst was easily and rapidly separated from the reaction

mixture using an external magnet and washed with diethyl ether to remove residual product, then reused for the next run under the same reaction conditions as for the first run. As shown in Figure 8, the  $\text{Fe}_3\text{O}_4\text{@MCM-41@Pd-SPATB}$  can be recycled for at least five runs without any significant loss of its catalytic activity or palladium leaching.

Finally, hot filtration test was investigated to check if the leached metal species are responsible for the catalytic activity in Suzuki reaction iodobenzene with phenylboronic acid as a model substrate in the presence of  $\text{Fe}_3\text{O}_4\text{@MCM-41@Pd-SPATB}$  (4 mg, 0.64 mol%) at 80 °C in PEG-400. In this experiment the product was obtained after 13 min (in the half time of the reaction) in 62% yield. Then the reaction was repeated but in the half time of the reaction (after 13 min), the catalyst was separated from the reaction mixture and the reaction mixture was allowed to run for another 13 min. The yield of reaction in this stage is 64% that confirmed the leaching of palladium during the reaction hasn't been occurred.

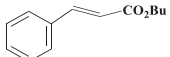
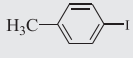
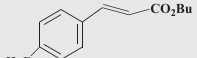
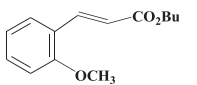
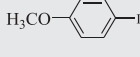
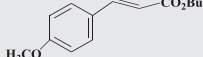
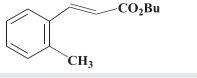
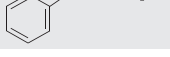
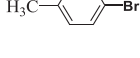
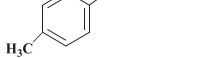
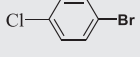
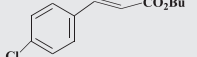
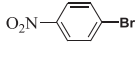
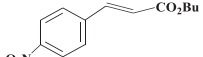
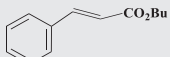
Also, to measure the exact leaching of palladium in the catalyst, the amount of palladium in  $\text{Fe}_3\text{O}_4\text{@MCM-41@Pd-SPATB}$  was determined using ICP-OES after five recycles. The amount of Pd in catalyst was found to be  $1.54 \times 10^{-3}$  mol/g based on ICP-OES for catalyst after 5 runs reused. Therefore the catalyst can be recovered and reused without any significant leaching Pd. The results from hot filtration test and ICP-OES technique show that leaching of palladium during the reaction is negligible.

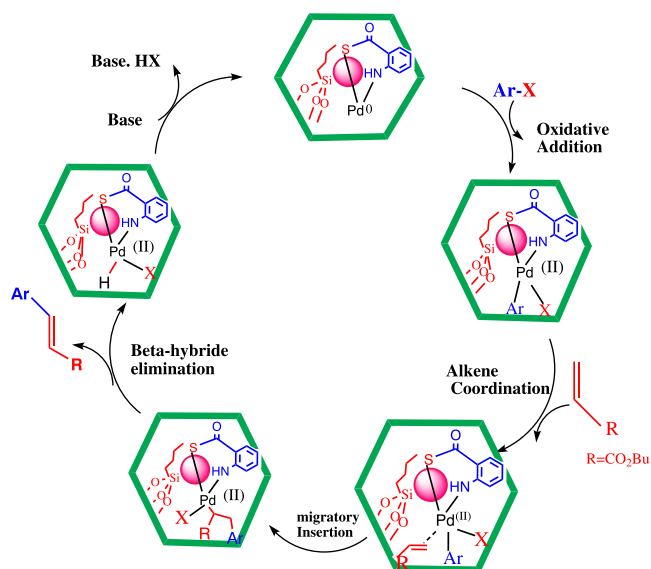
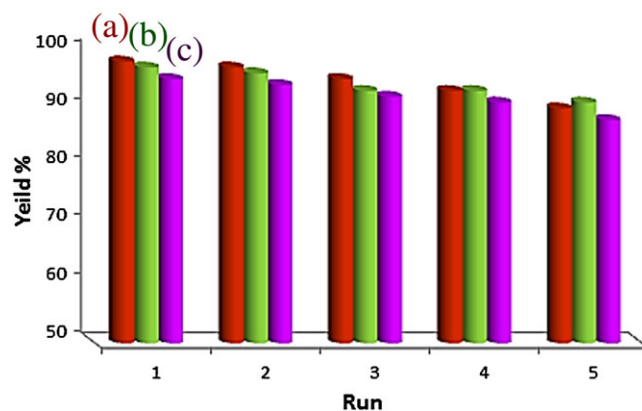
**TABLE 5** Catalytic results for the heck reaction

Entry	Temperature (°C)	Solvent	Base	Catalyst (mg)	Time (min)	Yield (%) <sup>b</sup>
1	120	PEG-400	$\text{K}_2\text{CO}_3$	None	24 <sup>a</sup>	Trace
2	120	PEG-400	$\text{K}_2\text{CO}_3$	3	30	62
3	120	PEG-400	$\text{K}_2\text{CO}_3$	4	30	85
4	120	PEG-400	$\text{K}_2\text{CO}_3$	6	30	92
5	120	PEG-400	$\text{NaHCO}_3$	6	30	76
6	120	PEG-400	$\text{Et}_3\text{N}$	6	30	88
7	120	PEG-400	$\text{KOH}$	6	30	45
8	120	PEG-400	$\text{Na}_2\text{CO}_3$	6	30	85
9	120	Toluene	$\text{K}_2\text{CO}_3$	6	30	-
10	120	DMSO	$\text{K}_2\text{CO}_3$	6	30	68
11	120	DMF	$\text{K}_2\text{CO}_3$	6	30	84
12	120	$\text{H}_2\text{O}$	$\text{K}_2\text{CO}_3$	6	30	-
13	120	$\text{EtOH}$	$\text{K}_2\text{CO}_3$	6	30	84
14	110	PEG-400	$\text{K}_2\text{CO}_3$	6	30	86
15	100	PEG-400	$\text{K}_2\text{CO}_3$	6	30	68
16	80	PEG-400	$\text{K}_2\text{CO}_3$	6	30	52

Reaction conditions: aryl halide (1 mmol), *n*-butyl acrylate (1.2 mmol), base (3 mmol),  $\text{Fe}_3\text{O}_4\text{@MCM-41@Pd-SPATB}$  (6 mg), and PEG-400 (2 ml).

**TABLE 6** The heck reaction of aryl halides with *n*-butyl acrylate using heterogeneous Fe<sub>3</sub>O<sub>4</sub>@MCM-41@Pd-SPATB catalyst (0.94 mol%) at 120°C in PEG-400

$\text{R}_1\text{-C}_6\text{H}_4\text{-X} + \text{CH}_2=\text{CH-CO}_2\text{Bu} \xrightarrow[\text{K}_2\text{CO}_3, \text{PEG}, 120^\circ\text{C}]{\text{Fe}_3\text{O}_4\text{@MCM-41@Pd-SPATB}} \text{R}_1\text{-C}_6\text{H}_4\text{-CH=CH-CO}_2\text{Bu}$ <p style="text-align: center;">X=Br, Cl, I</p>						
Entry	Substrate	Product	Time (min)	Yield (%) <sup>a</sup>	TOF (h <sup>-1</sup> )	Melting point (°C)
1			30	92	195.7	Oil [25]
2			40	90	145.06	Oil [25]
3			90	86	60.9	Oil [25]
4			40	91	145.3	Oil [25]
5			90	89	63.1	Oil [25]
6			100	86	54.9	Oil [25]
7			100	81	51.7	Oil [25]
8			120	87	46.2	Oil [26]
9			90	90	63.8	40-43 [27]
10			360	86	15.2	Oil [25]

<sup>a</sup>Isolated yield.**SCHEME 3** Possible mechanism of Heck coupling reactions**FIGURE 8** Reusability of Fe<sub>3</sub>O<sub>4</sub>@MCM-41@Pd-SPATB catalyst for the Suzuki (column a), Stille (column b) and Heck cross-coupling reactions (column c)

**TABLE 7** Comparison of the effect of Fe<sub>3</sub>O<sub>4</sub>@MCM-41@Pd-SPATB with other catalysts for Suzuki–Miyaura reaction using iodobenzene and phenylboronic acid

Entry	Catalyst (mol% of Pd)	Conditions	Time (h)	TOF (h <sup>-1</sup> )	Yield (%)	Ref.
1	Pd-imino-Py-γ-Fe <sub>2</sub> O <sub>3</sub> (0.25 mol%)	Et <sub>3</sub> N, DMF, 100 °C	0.5	760	95	[33]
2	Fe <sub>3</sub> O <sub>4</sub> /DAG/Pd(0.2 mol%)	K <sub>2</sub> CO <sub>3</sub> , EtOH/ H <sub>2</sub> O, 25 °C	0.16	3062	98	[34]
3	Pd@Cu-BDC/Py-SI MOF(0.2 mol%)	K <sub>2</sub> CO <sub>3</sub> , DMF/ H <sub>2</sub> O, 80 °C	0.5	1000	100	[35]
4	Pd-Py-MCM-41(1.56 mol%)	Na <sub>2</sub> CO <sub>3</sub> , PEG, 80 °C	2	31.08	97	[36]
5	MCM-41-S-Pd(0) (0.5 mol%)	K <sub>2</sub> CO <sub>3</sub> ,DMF-H <sub>2</sub> O, 80 °C	6	32.6	98	[37]
6	MOF-253-0.05PdCl <sub>2</sub> (0.23 mol%)	KOAc, DMF:EtOH, 100 °C	8	53.2	98	[38]
7	@Pd/meso-TiO <sub>2</sub> /Pd@meso-SiO <sub>2</sub> (0.04 mol%)	Cs <sub>2</sub> CO <sub>3</sub> , EtOH, 80 °C	0.16	15 390	99	[39]
8	m-6,6'-Me <sub>2</sub> bpy-MOF-PdCl <sub>2</sub> (1 mol%)	K <sub>2</sub> CO <sub>3</sub> , Toluene, 85 °C	12	8.25	99	[40]
9	Fe <sub>3</sub> O <sub>4</sub> @MCM-41@Pd-SPATB(0.63 mol%)	K <sub>2</sub> CO <sub>3</sub> , PEG, 80 °C	0.41	355.2	94	This work

**TABLE 8** Comparison of the effect of Fe<sub>3</sub>O<sub>4</sub>@MCM-41@Pd-SPATB with other catalysts for heck–Mizoroki cross-coupling reactions using iodobenzene and buthyl acrylate

Entry	Catalyst (mol% of Pd)	Conditions	Time (h)	TOF (h <sup>-1</sup> )	Yield (%)	Ref.
1	Fe <sub>3</sub> O <sub>4</sub> @SiO <sub>2</sub> /Schiff base/Pd(II) (0.3 mol%)	K <sub>2</sub> CO <sub>3</sub> , DMF, 110 °C	0.75	430	97	[41]
2	Pd/Fe <sub>3</sub> O <sub>4</sub> @PIL-NH <sub>2</sub> (0.011 mol%)	Et <sub>3</sub> N, 120 °C	0.66	12682	93	[42]
3	SiO <sub>2</sub> @Fe <sub>3</sub> O <sub>4</sub> -Pd (1 mol%)	K <sub>2</sub> CO <sub>3</sub> , DMF, 100 °C	8	12.1	97	[43]
4	Pd@MIL-101 (0.15 mol%)	K <sub>2</sub> CO <sub>3</sub> , DMF, 120 °C	2	330	99	[44]
5	Pd(OAc) <sub>2</sub> @MNP (0.5 mol%)	Et <sub>3</sub> N, DMF, 100 °C	1.5	128	96	[45]
6	NHC-Pd(II) (1 mol%)	Na <sub>2</sub> CO <sub>3</sub> , DMA, 160 °C	18	5.5	99	[46]
7	Pd/Fe <sub>3</sub> O <sub>4</sub> (5 mol%)	K <sub>2</sub> CO <sub>3</sub> , NMP, 130 °C	5	3.96	99	[47]
8	Fe <sub>3</sub> O <sub>4</sub> /DAG/Pd (0.3 mol%)	Et <sub>3</sub> N, DMF, 110 °C	0.5	640	96	[48]
9	Fe <sub>3</sub> O <sub>4</sub> @MCM-41@Pd-SPATB (0.94 mol%)	K <sub>2</sub> CO <sub>3</sub> , PEG, 120 °C	0.5	195.7	92	This work

In the next study, in order to compare the catalytic potentiality of Fe<sub>3</sub>O<sub>4</sub>@MCM-41@Pd-SPATB with the reported catalysts in the literature, we compared the results of the coupling of iodobenzene with phenylboronic acid (Table 7) and iodobenzene with buthyl acrylate (Table 8) with the previously reported methods. As shown in Table 7 and 8, in this work, C–C bond forming reaction has been carried out in PEG-400 as green solvent and this catalyst shows shorter reaction time and higher yield than the other catalysts. Especially this new catalyst also is a proper catalyst in terms of stability, non-toxicity, price and easy separation than the previously reported ones. In addition, the recyclability of this catalyst is faster and easier than those of the other reported catalysts.

## 4 | CONCLUSION

In summary, Pd(0)- S-propyl-2-aminobenzothioate immobilized onto functionalized magnetic nanoporous

MCM-41 has been prepared and fully characterized using FT-IR, XRD, VSM, EDS, SEM, TEM and TGA techniques, and successfully used as efficient and recyclable nanocatalyst for the Suzuki, Still and Heck reactions under mild experimental conditions. The given simple experimental procedure in this work, avoided the use of organic solvents which is in agreement with green chemistry principles, utilization of an inexpensive and readily available catalyst, good reactivity to generate the corresponding products in good to excellent yields for all reactions are the advantages of the present method. In addition, this catalyst was easily separable from the reaction mixture by external magnet and can be reused for five runs without any significant loss of stability and activity.

## ACKNOWLEDGMENT

The authors gratefully acknowledge Ilam University Research Council for partial financial support of this study.

## ORCID

Mohsen Nikoorazm  <http://orcid.org/0000-0002-4013-0868>  
 Arash Ghorbani-Choghamarani  <http://orcid.org/0000-0002-7212-1317>

## REFERENCES

- [1] A. Ghorbani-Choghamarani, B. Tahmasbi, P. Moradi, *Appl. Organometal. Chem.* **2016**, 30(6), 422.
- [2] S. Islam, A. Roy, P. Mondal, N. Salam, *App. Organomet. Chem.* **2012**, 26, 625.
- [3] Y. He, C. Cai, *Appl. Organometal. Chem.* **2011**, 25, 799.
- [4] S. Nadri, M. Joshaghani, E. Rafiee, *Appl. Catal. A.* **2009**, 362, 163.
- [5] S. Pasa, Y. S. Ocak, H. Temel, T. Kilicoglu, *Inorg. Chim. Acta.* **2013**, 405, 493.
- [6] A. R. Hajipour, F. Rafiee, *J. Iran. Chem. Soc.* **2015**, 12, 1177.
- [7] Y. J. Shang, J. W. Wu, C. L. Fan, J. S. Hu, B. Y. Lu, *J. Organomet. Chem.* **2008**, 693, 2963.
- [8] Y. Li, Y. Dai, Z. Yang, T. Li, *Inorg. Chim. Acta.* **2014**, 414, 59.
- [9] D. J. Cole-Hamilton, *Science* **2003**, 299, 1702.
- [10] A. F. Littke, G. C. Fu, *Angew. Chem., Int. Ed.* **2002**, 41, 4176.
- [11] A. Ghorbani-Choghamarani, M. Norouzi, *J. Mol. Catal. A: Chem.* **2014**, 395, 172.
- [12] U. Laska, C. G. Frost, G. J. Price, P. K. Plucinski, *J. Catal.* **2009**, 268, 318.
- [13] A. Ghorbani-Choghamarani, Z. Darvishnejad, B. Tahmasbi, *Inorg. Chim. Acta.* **2015**, 435, 223.
- [14] M. Hajjami, B. Tahmasbi, *RSC Adv.* **2015**, 5, 59194.
- [15] A. Ghorbani-Choghamarani, B. Tahmasbi, F. Arghand, S. Faryadi, *RSC Adv.* **2015**, 5, 92174.
- [16] M. Hasanzadeh, M. Pournaghi-Azar, N. Shadjou, A. Jouyban, *RSC Adv.* **2014**, 4, 4710.
- [17] M. Nikoorazm, A. Ghorbani-Choghamaran, N. Noori, *J Porous Mater* **2015**, 22, 877.
- [18] Z. Abbasi, S. Rezayati, M. Bagheri, R. Hajinasiri, *Chin. Chem. Letter.* **2017**, 28, 75.
- [19] M. Abdollahi-Alibeik, A. Rezaeipoor-Anari, *J. Magn. Magn. Mater.* **2016**, 398, 205.
- [20] M. Arruebo, W. Yan Ho, K. Fung Lam, X. Chen, J. Arbiol, J. Santamaría, K. Lun Yeung, *Chem. Mater.* **2008**, 20, 486.
- [21] M. Nikoorazm, F. Ghorbani, A. Ghorbani-Choghamarani, Z. Erfani, *Chine. J. catal.* **2017**, 38, 1413.
- [22] A. Ghorbani-Choghamarani, H. Rabiei, *Tetrahedron Lett.* **2016**, 57, 159.
- [23] Y. Peng, J. Liu, X. Lei, Z. Yin, *Green. Chem.* **2010**, 12, 1072.
- [24] M. Gholinejad, H. R. Shahsavari, *Inorg. Chim. Acta.* **2014**, 421, 433.
- [25] Q. Xu, W. Duan, Z. Lei, Z. Zhu, M. Shi, *Tetrahedron.* **2005**, 61, 11225.
- [26] N. Iranpoor, H. Firouzabadi, A. Tarassoli, M. Fereidoonzhad, *Tetrahedron.* **2010**, 66, 2415.
- [27] A. Naghipour, A. Fakhri, *Catalysis Communications* **2016**, 73, 39.
- [28] S. Navaladian, B. Viswanathan, T. K. Varadarajan, R. P. Viswanath, *Nanoscale Res. Lett.* **2009**, 4, 181.
- [29] L. Zhou, Z. WeiDe, J. HuanFeng, *Sci. China Chem.* **2008**, 51, 241.
- [30] M. Nikoorazm, A. Ghorbani-Choghamarani, N. Noori, *Res. Chem. Intermediates.* **2016**, 42(5), 4621.
- [31] L. Douglas, A. Osvaldo, Y. Iamamoto, *Microporous and Mesoporous Mater.* **2016**, 219, 161.
- [32] S. Rostamizadeh, M. Nojavan, R. Aryan, M. Azad, *Catal Lett.* **2014**, 144, 1772.
- [33] S. Sobhani, Z. Mesbah Falatoooni, S. Asadi, M. Honarmand, *Catal. Lett.* **2016**, 146, 255.
- [34] H. Veisi, J. Gholami, H. Ueda, P. Mohammadi, M. Noroozi, *J. Mol. Catal. A: Chem.* **2015**, 396, 216.
- [35] S. Rostamnia, H. Alamgholiloo, X. Liu, *J. colloid and interface science* **2016**, 469, 310.
- [36] M. Nikoorazm, A. Ghorbani-Choghamarani, A. Jabbari, *J Porous Mater* **2016**, 23, 967.
- [37] M. Cai, Q. Xu, Y. Huang, *J. Mol. Catal. A Chem.* **2007**, 271, 93.
- [38] L. Chen, Z. Gao, Y. I. Li, *Catalysis Today* **2015**, 245, 122.
- [39] B. Liu, Y. Niu, Y. Li, F. Yang, J. Guo, Q. Wang, P. Jing, J. Zhang, G. Yun, *Chem. Commun.* **2014**, 50, 12356.
- [40] X. Li, R. Van Zeeland, R. V. Maligal-Ganesh, Y. Pei, G. Power, L. Stanley, W. Huang, *ACS Catalysis* **2016**, 6, 6324.
- [41] M. Esmaeilpour, J. Javidi, *J. Chin. Chem.* **2015**, 62(7), 614.
- [42] W. Liu, D. Wang, Y. Duan, Y. Zhang, F. Bian, *Tetrahedron. Lett* **2015**, 56, 1784.
- [43] P. H. Li, L. Wang, L. Zhang, G. W. Wang, *Adv. Synth. Catal.* **2012**, 354, 1307.
- [44] N. Shang, S. Gao, X. Zhou, C. Feng, Z. Wang, C. Wang, *RSC Adv.* **2014**, 4, 54487.
- [45] Z. Qiang, X. Zhao, H. Wei, J. Li, J. Luo, *Appl. Organomet. Chem.* **2016**, <https://doi.org/10.1002/aoc.3608>.
- [46] T. Chen, J. Gao, M. Shia, *Tetrahedron* **2006**, 62, 6289.
- [47] F. Zhang, J. Niu, H. Wang, H. Yang, J. Jin, N. Liu, Y. Zhang, R. Li, J. Ma, *Materials Research Bulletin.* **2012**, 47, 504.
- [48] H. Veisi, A. Sedrpoushan, S. Hemmati, *Appl. Organomet. Chem.* **2015**, 12, 825.
- [49] X. Chen, J. Jiang, F. Yan, S. Tiana, K. Li, *RSC Adv.* **2014**, 4, 8703.

**How to cite this article:** Nikoorazm M, Ghorbani F, Ghorbani-Choghamarani A, Erfani Z. Pd(0)- S-propyl-2-aminobenzothioate immobilized onto functionalized magnetic nanoporous MCM-41 as efficient and recyclable nanocatalyst for the Suzuki, Stille and Heck cross coupling reactions. *Appl Organometal Chem.* 2018;e4282. <https://doi.org/10.1002/aoc.4282>